

# COMPARISON OF REAL AND COMPLEX-VALUED VERSIONS OF WAVELET TRANSFORM, CURVELET TRANSFORM AND RIDGELET TRANSFORM FOR MEDICAL IMAGE DENOISING

Huseyin YASAR<sup>1</sup>, Murat CEYLAN<sup>2</sup>, Ayse Elif OZTURK<sup>3</sup>

<sup>1</sup>Ministry of Health, Ankara, TURKEY, E-mail: mirhendise@gmail.com

<sup>2</sup>Selcuk University, Department of Electrical and Electronics Engineering, 42075, Konya,  
TURKEY, E-mail: mceylan@selcuk.edu.tr

<sup>3</sup>Istanbul Aydin University, Electronics Technology, 34295, Kucukcekmece, Istanbul,  
TURKEY, Corresponding Author's E-mail: ayseozturk@aydin.edu.tr

**Abstract-** In this study; medical images were denoising with multiresolution analyses using real-valued wavelet transform (RVWT), complex-valued wavelet transform (CVWT), ridgelet transform (RT), real-valued first-generation curvelet transform (RVFG CT), real-valued second-generation curvelet transform (RVSG CT), complex-valued second-generation curvelet transform (CVSG CT) and results are compared. First and second-generation curvelet transformations are used for real-valued curvelet transform as two techniques. For the evaluation of the proposed system, we used 32 lung CT images. These images include 10 images with benign nodules and 22 images with malign nodules. Different types of noise like the Random noise, Gaussian noise and Salt & Pepper noise were added to these images and they are removed separately. The performances of used transforms are compared using Peak Signal to Noise Ratio (PSNR) parameter. Obtained results showed that complex-valued wavelet transform are suited for removal of random noise and Gaussian noise. In case of Gaussian noise in images, PSNRs of first generation curvelet transform and complex-valued wavelet transform are around 33 dB. The ridgelet transform provides high PSNR value (30.4dB) for denoising of salt & pepper noise in images.

**Key Words:** Wavelet transform, curvelet transform, ridgelet transform, denoising

## 1. INTRODUCTION

Image processing is an engineering discipline that has been studied extensively and also contains obtaining new images by analyzing the various images. The importance of image processing, especially after digital image recording's being widespread, has been increasing day by day. Image processing techniques are used a wide variety of fields like face / fingerprint identification security systems, electromagnetic radar systems, medical systems, geology and astronomy research, mapping and control systems. Fourier analysis which is used for obtaining the information about frequency of image is the basic argument of image processing. Since it is unknown that which or when signals are active, some problems can be occur while implementing the process conversely to unstable frequency valued signals. On the other hand, there

is no problem with the signals have time-invariant frequency value.

Since Fourier analysis is inefficient in time-frequency plane, wavelet analysis which is the basic of multi-resolution analysis is detected. Continuous wavelet analysis is firstly implemented in field of geophysics in 1982 by Morlet [1]. Although Grossman and Morlet [2] studied on this subject in 1984, basic wavelet transform developed by Chui [3] in 1992 and Meyer [4] in 1993. Discrete form of this analysis is improved by Mallat[5] in 1989 and Daubechies [6] in 1992. Wavelet package analysis is the complex form of discrete wavelet analysis and formed by Coifman and Wickerhauser [7] in 1992. It is proved that wavelets have complex solutions by Lawton [8] in 1993 and Lina [9] in 1997. First applications of wavelet analysis about noise removal is implemented for uni-dimensional signals by Lang et. al. [10]. In 1996, wavelet

analysis began to be implemented on medical images with the study of Mojsilovic et. al. [11]. Studies of Chang et. al. [12] in 2000 was about noise removal for wavelet transform on two-dimensional images. Some other scientists studied on denoising with wavelet transform as Portilla et. al. [13], Chen and Bui [14], Abdulmunim [15] and Benjaminsen [16] who used complex valued wavelet transform to remove noises in 2007.

Wavelet transform is suitable to use for identifying the images but this transform can only be used for horizontal, vertical or diagonal ( $45^\circ$ ). Because of this restrictive situation, changes on the other angle block is ignored, thus Ridgelet transform is developed by Candes and Donoho [17] to get over this problem. The difference between Ridgelet and wavelet analyses is that angular windows are identified in Ridgelet analysis and so images can be expressed with much and effective coefficients. Ridgelet transform is firstly used for removing noise by Do and Vetterli [18].

Curvelet analysis is based on wavelet analysis but uses curves not lines like wavelet for windowing. Curvelet analysis came out in 1999 by Candes and Donoho [19] and it is built up on Ridgelet analysis. Donoho et. al. developed this analysis's digital [20] and discrete [21] versions in time. Starck[22] established that Curvelet analysis is more suitable to find images' edge regions. Starck et. al. used Curvelet transform to remove noises in 2002. Also Gyaourova et. al. [23] studied on this subject in the same year. In 2007, Sivakumar [24] removed noises from CT images. A similar study is gone over in 2010 by Rayudu et. al. [25].

Although real types of transforms are used for denoising noises many times individually, there are really a few studies use some of them with or compare them with the each other. In addition, usually just one type noise is implemented to image and then it is removed in these studies. Number of the studies about performance evaluations for more than one noise is really a few. Studies about complex-valued wavelet and complex curvelet transform keep developing.

In this study, a denoising application is implemented on CT lung images with three type of noise using real-valued and complex-valued wavelet transforms, ridgelet transform, first and second-generation curvelet transforms and denoising algorithms. PSNR value is calculated between acquired images and original images.

## 2. METHOD

### 2.1. Wavelet Transform

Wavelet is a useful tool for representing nonlinearity [26]. A function  $f(x)$  can be symbolized by the superposition of daughters  $a, b$

$(x)$  of a mother wavelet  $(x)$ . Where  $a, b(x)$  can be denoted as

$$\mathbb{E}(a, b)(x) = \frac{1}{\sqrt{a}} \mathbb{E}\left(\frac{x-b}{a}\right) \quad (1)$$

$a \in \mathbb{R}_+$  and  $b \in \mathbb{R}$  are, separately, called dilation and translation parameters. The continuous wavelet transform of  $f(x)$  is described as

$$\mathbb{E}(a, b) = \int_{\mathbb{R}^2} f(x) \mathbb{E}_{a, b}(x) . d(x) \quad (2)$$

and the function  $f(x)$  can be reconstructed by the reverse wavelet transform

$$f(x) = \int \int_{-\infty}^{\infty} w(a, b) \mathbb{E}_{a, b}(x) . \frac{da . db}{a^2} \quad (3)$$

The continuous wavelet transform and its inverse transform are not suitable to implement directly on digital computers. When the reverse wavelet transform is discretized,  $f(x)$  has the following approach wavelet-based representation form:

$$\hat{f}(x) \approx \sum_{k=1}^K w_k \mathbb{E}\left(\frac{x-b_k}{a_k}\right) \quad (4)$$

where the  $w_k$ ,  $b_k$  and  $a_k$  are weight coefficients, translations and dilations for each daughter wavelet [26]. It is perceived that the wavelet transform is an significant tool for analysis and processing of signals and images. In spite of its efficient computational algorithm, the wavelet transform suffers from three essential disadvantages: shift sensitivity, poor directionality and absence of phase information [27-32].

Most DWT applications use sectional filtering with real coefficient filters associated with real wavelets resulting in real-valued approximations and details. Such DWT implementations cannot ensure the local phase information. All natural signal are fundamentally real-valued, hence to avoid the local phase information, complex-valued filtering is necessary [33, 34]. Latest research in the improvement of complex wavelet transforms (CWTs) can be broadly classified in two groups; RCWT (Redundant CWTs) and NRCWT (Non-redundant CWTs). The RCWT contains two almost similar CWTs. They are denoted as DT-DWT (Dual-Tree DWT based CWT, see Figure 1) with two almost similar models namely Kingsbury's and Selesnick's [35]. In this paper, we used Kingsbury's CWT [34, 36] for image denoising.

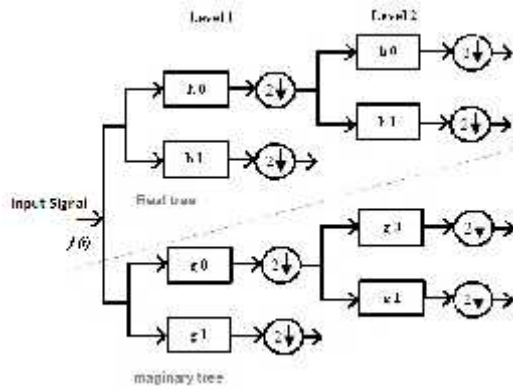


Figure 1: Complex Wavelet Transform with two level

## 2.2. Ridgelet Transform

The achievement of the wavelets essentially depends on the good performance brought by the one-dimensional (1-D) piecewise smooth functions. Unfortunately, this success is not acceptable in the two-dimensional (2-D) case. Fundamentally, wavelets are good at catching zero-dimensional or point singularities. However, 2-D signals (i.e., images) generally include 1-D singularities (i.e., edges and corners). The edges separate the smooth regions by creating discontinuity across the edge while the edges themselves are also regular along the edge. By sentence, 2-D wavelet transforms are created by the tensor products of 1-D

wavelets and they will so isolate the discontinuity across the edge by missing the smoothness along the edge.

In order to get over the weakness of wavelet transform in two or more dimensions, Candès and Donoho [17] improved a new system of representations called “ridgelets” which can effectively cover the line singularities in two dimensions. Nowadays, Ridgelets have been applied in image processing [37,38]. For each  $a > 0$ , each  $b \in \mathbb{R}$  and each  $\theta \in [0, 2\pi]$ , the bivariate ridgelet  $\Psi_{a,b,\theta} : \mathbb{R}^2 \rightarrow \mathbb{R}$  is described as

$$\Psi_{a,b,\theta}(x) = a^{-1/2} \mathcal{E}((x_1 \cdot \cos \theta + x_2 \cdot \sin \theta - b) / a) \quad (5)$$

A ridgelet is stable along the lines  $x_1 \cos \theta + x_2 \sin \theta = \text{constant}$ . Transverse to these ridges it is a wavelet and given an integrable bivariate image  $f(x_1, x_2)$ , we can describe its ridgelet coefficients as

$$R(a, b, \theta) = \int \mathcal{E}_{a,b,\theta} \cdot f(x_1, x_2) dx_1 dx_2 \quad (6)$$

The ridgelet transform can be indicated in terms of the Radon transform. The Radon transform of an image  $f(x_1, x_2)$  is described as

$$RA(\theta, t) = \int f(x_1, x_2) \delta(x_1 \cdot \cos \theta + x_2 \cdot \sin \theta - t) dx_1 dx_2 \quad (7)$$

where  $\delta$  is the Dirac distribution.

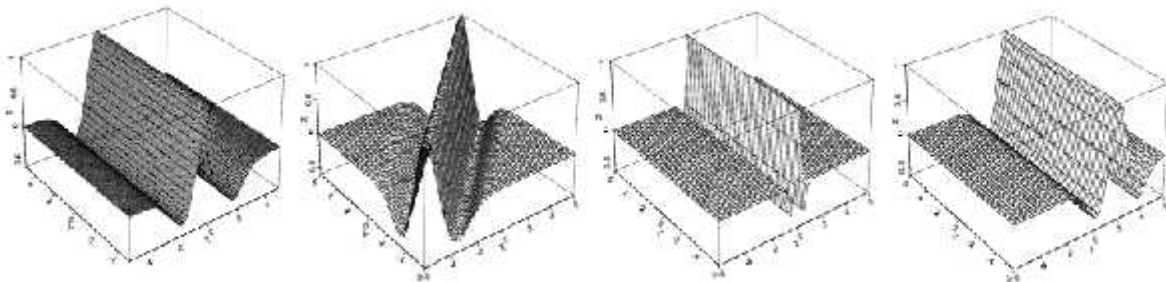


Figure 2: Ridgelet samples

Thus the ridgelet transform is precisely the implementation of a 1D wavelet transform to the slices of the Radon transform where the angular variable  $\theta$  is stable and  $t$  is varying. Ridgelets are different from wavelets in a sense that ridgelets exhibit so high directional susceptibility and are highly anisotropic. A fast ridgelet transform can be applied in the Fourier domain. The 2D FFT is computed firstly. Then it is interpolated along a few straight lines equal to the selected number of projections. Each line passes through the centre of the 2D frequency space, with an inclination equal to

the projection angle, and a number of interpolation points equal to the number of rays per projection. After the 1D reverse FFT along each interpolated ray, we perform a 1D wavelet transform. Pay attention to that the ridgelet coefficients so obtained are not represented in the Fourier frequency domain. The Fourier transform used is only a tool to succeed a fast application of the ridgelet transformation. Actually, it is equivalent to applying 1D wavelet transform to the Radon slices of the original pattern image.

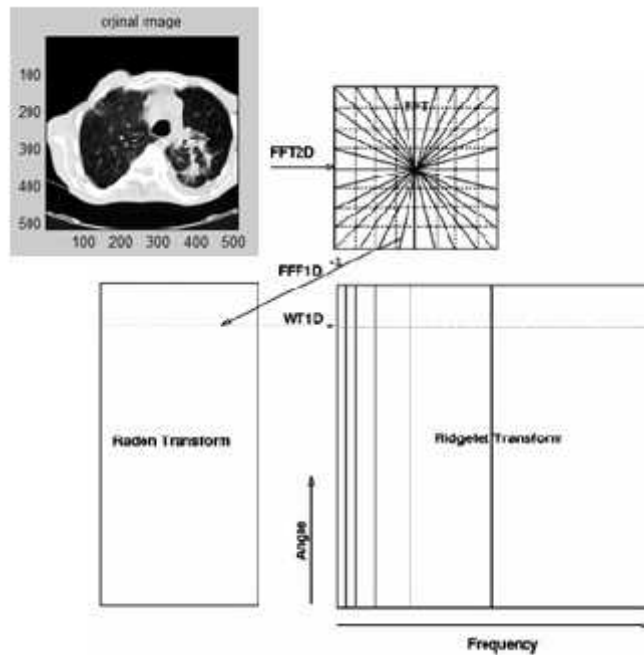


Figure 3: Scheme of ridgelet transform

### 2.3. Curvelet Transform

The idea of curvelets is to represent a curve as a superposition of functions of a variety of lengths and widths corresponding the scaling law  $width \propto length^2$  [19]. This can be done by decomposing the image into subbands firstly, i.e., separating the object into series of disjoint scales. Each scale is then evaluated by means of a local ridgelet transform. Curvelets are based on multiscale ridgelets combined with a spatial bandpass filtering process to isolate different scales. This spatial bandpass filter nearly kills all multiscale ridgelets which are not in filter's frequency range. In other words, a curvelet is a kind of multiscale ridgelet which lives in a prescribed frequency band. The bandpass is set so the curvelet length and width at fine scales are interrelated by a scaling law  $width \propto length^2$  and so the anisotropy increases with decreasing scale like a power law. There is a very special correlation between the index of the dyadic subbands and the depth of the multiscale pyramid; the edge length of the localizing windows is doubled at per other dyadic subband, thus maintaining the fundamental property of the curvelet transform which says that elements of length about  $2^{-j}$  serve for the analysis and synthesis of the  $j$  th subband  $[2^j, 2^{j+1}]$ . Curvelets have a scaling corresponding  $width \propto length^2$  while multiscale ridgelets have random dyadic length and random dyadic widths. Loosely speaking, the curvelet dictionary is a subset of the multiscale ridgelet dictionary, however which allows reconstruction.

The discrete curvelet transform of a continuous function  $f(x_1, x_2)$  makes use of a dyadic sequence of scales, and a bank of filters  $(P_0 f, \Delta_1 f, \Delta_2 f)$  with the feature that the passband filter  $s$  is concentrated near the frequencies  $[2^{2s}, 2^{2s+2}]$ , e.g.,

$$P_0 f = \Phi_Q x f, \quad \Delta_s f = \Psi_{2^s} x f \quad (8)$$

In wavelet theory, a decomposition into dyadic subbands  $[2^s, 2^{s+1}]$  is used. Contrarily, the subbands used in the discrete curvelet transform of continuum functions have the non-standard form  $[2^{2s}, 2^{2s+2}]$ . This is non-standard characteristic of the discrete curvelet transform well worth considering. The curvelet decomposition is the sequence of the following steps with the notations of section above,

*Subband Decomposition.*  $f$  is decomposed into subbands

$$f = (P_0 f, \Delta_1 f, \Delta_2 f, \Delta_3 f) \quad (9)$$

*Smooth Partitioning.* Each subband is smoothly windowed into an appropriate scale's "squares" (sidelength  $2^{-s}$ )

$$\Delta_s f = (w_Q \cdot \Delta_s f)_{Q \in Q_s} \quad (10)$$

*Renormalization.* Each resulting square is renormalized to unit scale

$$g_0 = T_Q^{-1} \cdot (w_Q \cdot \Delta_s f)_{Q \in Q_s} \quad (11)$$

*Ridgelet Analysis.* The discrete ridgelet transform is used for analysing each square. In the definition, the ridgelet transform is applied after the two dyadic subbands  $[2^{2s}, 2^{2s+1}]$  and  $[2^{2s+1}, 2^{2s+2}]$  are merged.

We proposed a non-aliasing Curvelet transform to overcome the aliasing in Curvelet transform, namely complex Curvelet transform. The key innovation can be universalized as follows: 2D and 1D complex wavelet transform.

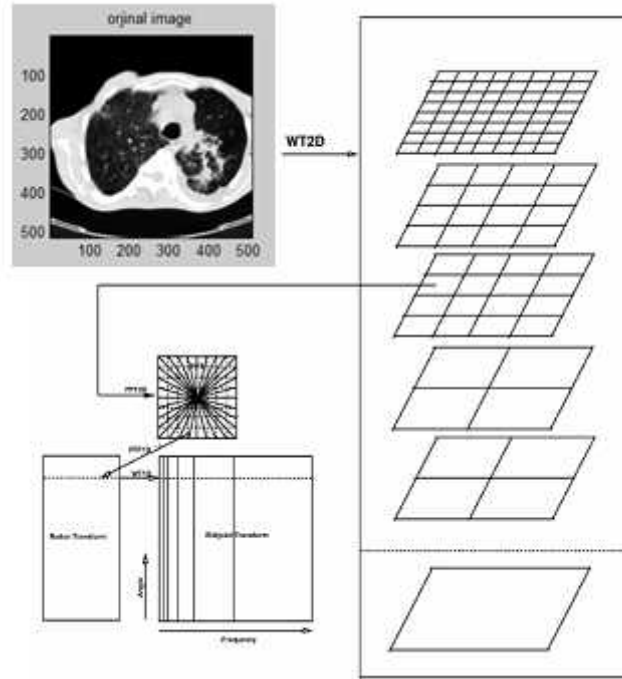


Figure 4: Scheme of curvelet transform

#### 2.4. Peak Signal-to-Noise Ratio (PSNR)

Any processing implemented to an image may cause an significant loss of information or quality. Image quality estimation methods can be subdivided into objective and subjective methods [37, 38]. Subjective ways are based on human judgment and operate without reference to explicit criteria [39]. Objective ways are based on comparisons using explicit numerical criteria [40, 41], and several references are feasible such as the ground truth or prior knowledge expressed in terms of statistical parameters and tests [42, 43]. Given a reference image  $f$  and a test image  $g$ , both  $M \times N$  sized, the PSNR between  $f$  and  $g$  is defined by:

$$PSNR(f, g) = 10 \cdot \log_{10}(255^2 / MSE(f, g)) \quad (12)$$

$$MSE(f, g) = \frac{1}{MN} \cdot \sum_{i=1}^M \sum_{j=1}^N (f_{i,j} - g_{i,j})^2 \quad (13)$$

The PSNR value approaches infinity as the MSE approaches zero; this shows that a higher PSNR value provides a higher image quality. At the other tip of the scale, a small value of the PSNR implies high numerical distinctions between images.

#### 3. USED DATA

In this study, 32 CT images taken from Baskent University Konya Research Hospital are used. Image collection is labeled as benign or malign by an expert radiologist using biopsy reports. This labeled image database includes 32 images (12 benign and 20 malign nodules) [44].

#### 4. RESULTS AND DISCUSSION

Real-valued wavelet transform (RVWT), complex-valued wavelet transform (CVWT), ridgelet transform (RT), real-valued first-generation curvelet transform (RVFG CT), real-valued second-generation curvelet transform (RVSG CT), complex-valued second-generation curvelet transform (CVSG CT) are implemented on the images and their parameters are obtained. Random, gaussian, salt & pepper noises are implemented to

COMPARISON OF REAL AND COMPLEX-VALUED VERSIONS OF WAVELET TRANSFORM, CURVELET TRANSFORM AND RIDGELET TRANSFORM FOR MEDICAL IMAGE DENOISING

Huseyin YASAR, Murat CEYLAN, Ayse Elif OZTURK

the image. PSNR is calculated between the noisy image and the original image. These processes repeated one hundred times for all images. Averaged value of obtained results is calculated (see Table 1). In Table 1, B signify an image with benign nodule and M signify an image with malign nodule. According to Table 1, highest PSNR values for removal of random noise and Gaussian noise were obtained using CWT as 34.01 dB and 32.89

dB, respectively. In case of Gaussian noise in images, PSNRs of first generation curvelet transform and complex-valued wavelet transform are around 33 dB. The ridgelet transform provides high PSNR value (30.4dB) for denoising of salt & pepper noise in images. The resulting denoised output images for random selected input image (with benign nodule) are given in Figure 5, Figure 6 and Figure 7.

	PSNR Values For Random Noise						PSNR Values For Gaussian Noise						PSNR Values For Salt & Pepper Noise					
	FJWTF	CJWTF	RT	RJWTF	RJSGCT	CJSGCT	FJWTF	CJWTF	RT	RJWTF	RJSGCT	CJSGCT	FJWTF	CJWTF	RT	RJWTF	RJSGCT	CJSGCT
B-1	32.6440	33.3804	29.7225	33.6186	32.6241	32.2192	31.6766	32.5944	29.0836	32.5305	31.7935	31.4275	21.6932	21.7859	29.7502	21.6683	24.8049	24.7187
B-2	31.9158	33.1369	29.0001	32.4769	32.0771	32.0423	31.2559	32.0975	28.5439	31.9603	31.6726	31.2457	21.7974	21.3845	29.0325	21.7382	24.8637	24.7551
B-3	32.7411	33.9162	30.5530	33.6897	32.2749	32.2125	32.0522	32.9599	29.8751	32.3517	32.1010	31.7098	21.7313	21.7925	30.4082	21.6346	24.7078	24.5232
B-4	32.6215	33.7781	30.7543	33.5049	32.0378	32.3605	31.8384	32.7081	30.1070	32.5294	32.1469	31.6904	21.6930	21.7873	30.6573	21.6904	24.7158	24.5300
B-5	32.3137	34.5150	30.5254	34.3893	32.5113	33.1895	32.4565	33.3914	30.3421	33.3485	32.6352	32.3320	21.5905	21.5783	30.8384	21.5810	24.8154	24.7574
B-6	32.8857	34.0715	30.5412	34.1457	32.3355	33.0131	32.1423	33.0189	29.9814	33.1741	32.5376	32.2374	21.6678	21.7589	30.5065	21.6373	24.8809	24.3164
B-7	32.8750	34.2424	30.4325	34.3519	32.3952	33.0644	32.4325	33.5741	30.0253	33.5697	32.8725	32.5701	22.0005	22.0925	30.5251	21.9920	25.2639	25.1904
B-8	32.2431	34.3380	31.2372	34.0886	32.6538	32.3283	32.5505	33.0171	30.5271	32.3677	31.8235	31.4867	21.7013	21.7871	31.5005	21.6927	24.7248	24.5603
B-9	32.3210	34.5168	30.6900	34.6796	32.8219	33.4768	32.4168	33.1114	30.1158	33.4337	32.8206	32.4982	21.7670	21.8445	30.7750	21.7588	25.0709	25.0141
B-10	32.6348	34.7585	31.1489	34.9297	34.1011	33.7875	32.6483	33.2863	30.3976	33.5347	33.0205	32.6763	21.6850	21.7615	31.0917	21.6774	25.0144	24.9551
B-11	32.5439	34.5610	31.4396	34.6175	32.2672	32.3873	32.5596	33.6288	30.8345	33.5987	32.6434	32.3182	21.6634	21.7465	31.3130	21.6343	24.7834	24.7237
B-12	32.8401	34.1292	30.5742	34.0895	32.5001	33.0747	32.1292	33.0174	29.8617	33.1484	32.6332	32.2571	21.5640	21.5571	30.2982	21.5340	24.7823	24.7128
M-1	32.6025	33.3643	30.1332	33.5121	32.5411	32.2295	31.8414	32.6270	29.5714	32.5789	31.8382	31.4958	21.6632	21.7604	30.1587	21.6396	24.8038	24.7343
M-2	32.8770	33.9145	30.4066	33.5311	32.1913	31.3054	31.9756	32.6689	29.8353	32.4775	31.4581	31.0742	21.5639	21.5605	30.3560	21.5306	24.4551	24.4333
M-3	32.1324	34.3321	30.5580	34.3004	32.8938	33.4631	32.1505	33.0553	30.2679	33.0903	32.8038	32.4422	21.7756	21.3555	30.5432	21.7567	25.0849	24.9669
M-4	31.8348	33.2893	29.1067	32.8764	32.1979	31.3282	31.3101	32.3636	28.6732	32.1303	31.5457	31.1256	21.8435	21.9475	29.1762	21.8340	24.8811	24.7759
M-5	32.1213	34.3133	30.8362	34.4461	32.8638	33.5059	32.3978	33.1582	30.2312	33.2621	32.5235	32.5367	21.5842	21.5673	30.8074	21.5551	24.7636	24.7104
M-6	32.2951	34.4913	31.0095	34.6402	34.1976	33.9165	32.5109	33.3180	30.4437	33.5665	33.2381	32.9154	21.6433	21.7183	31.0000	21.6343	24.9519	24.9001
M-7	32.3845	34.4272	31.5586	34.3518	32.0218	32.5857	32.2594	32.9028	30.4737	32.9494	31.5562	31.6582	21.5938	21.5851	31.3022	21.5899	24.7254	24.5727
M-8	32.9805	34.0843	30.6212	33.8284	32.5412	32.2135	32.2356	33.1675	30.2715	32.9554	31.9359	31.6105	21.9005	22.0015	30.6252	21.8911	24.9974	24.9157
M-9	32.8172	33.9902	30.7216	33.9751	32.5636	33.2333	32.0145	32.7400	30.0451	32.3300	32.5575	32.2136	21.5733	21.5669	30.6558	21.5389	24.7900	24.7303
M-10	32.4906	33.7935	29.6013	33.5462	32.8431	32.4051	31.6415	32.8128	29.3616	32.7895	32.2558	31.8398	21.8541	21.9488	29.6576	21.8442	25.0833	24.9471
M-11	32.8332	34.1350	30.2968	34.0518	32.2579	32.9781	32.0462	32.9038	29.6434	32.9161	32.3412	32.0387	21.6949	21.7740	30.2307	21.6858	24.9003	24.8340
M-12	32.9972	34.1533	30.8332	34.1314	32.5470	33.1622	32.3512	33.1885	30.3213	33.1270	32.6794	32.3039	21.8253	21.3959	30.5304	21.8172	25.0233	24.9521
M-13	32.2934	33.5768	29.5541	33.1792	32.4771	32.0654	31.4990	32.4508	29.0042	32.1913	31.6522	31.2345	21.8977	21.9824	29.6304	21.8694	24.9872	24.8820
M-14	32.2841	33.5473	29.7145	33.4039	32.0335	32.5039	31.7065	32.7756	29.3314	32.6300	32.3137	31.9184	21.8217	21.9215	29.7994	21.8125	25.0014	24.9155
M-15	32.6454	33.3185	30.4258	33.5106	32.1324	31.3577	31.8466	32.5991	29.8349	32.5119	31.4196	31.1022	21.8007	21.9052	30.4596	21.7903	24.8536	24.7723
M-16	32.6838	33.9235	30.1547	33.8071	32.1435	32.7727	31.7156	32.5172	29.4934	32.5464	32.1911	31.8194	21.5311	21.5132	30.0947	21.5126	24.6957	24.6345
M-17	32.5059	33.7602	29.6582	33.5375	32.8444	32.4465	31.8432	32.8566	29.4402	32.7725	32.2323	31.7952	21.8621	21.3563	29.6931	21.8327	25.0145	24.9234
M-18	32.1739	33.4131	29.6573	33.0453	32.4530	32.0033	31.2389	32.0144	29.1015	32.0025	31.5352	31.1337	21.5413	21.5310	29.6325	21.5325	24.5804	24.4971
M-19	32.3920	33.5082	29.7397	33.2149	32.0236	31.5737	31.7497	32.7353	29.2724	32.4674	31.4584	31.1357	21.8076	21.9043	29.7513	21.7989	24.8029	24.7250
M-20	32.7431	34.0070	30.3924	33.9105	32.1412	32.5950	32.0101	33.0747	29.8339	33.0343	32.4112	32.0122	21.7535	21.3450	30.3572	21.7307	24.9573	24.8753
Average	32.8030	34.0121	30.4160	33.8627	32.0803	32.5865	32.0547	32.8962	29.8417	32.8757	32.2399	31.8755	21.7217	21.8104	30.3909	21.7102	24.8639	24.7931

Table 1: Obtained results for medical image denoising process

COMPARISON OF REAL AND COMPLEX-VALUED VERSIONS OF WAVELET TRANSFORM, CURVELET TRANSFORM AND RIDGELET TRANSFORM FOR MEDICAL IMAGE DENOISING

Huseyin YASAR, Murat CEYLAN, Ayse Elif OZTURK

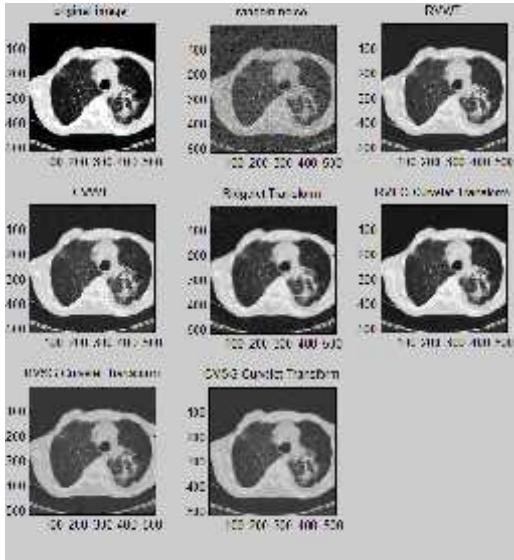


Figure 5: Denoised image outputs for *random noise* using multi-resolution analyses

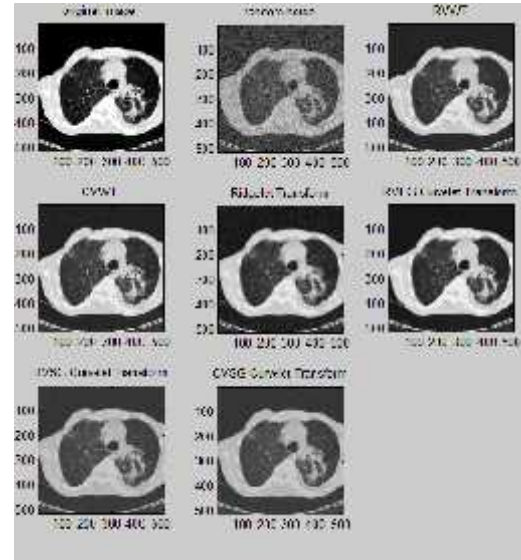


Figure 6: Denoised image outputs for *Gaussian noise* using multi-resolution analyses

5. CONCLUSIONS

In this study, multi-resolution analyses are implemented for medical image denoising and obtained results are concluded above:

- 1- Ability of defining images from best to worst is: curvelet transform, ridgelet transform, wavelet transform.
- 2- Denoising algorithm which is improved for ridgelet analysis did not provide the expected results for random noise and gaussian noise. On the other hand, although been worse than the other transformations, it was more useful for denoising salt&pepper.
- 3- For the future, multi-resolution analyses can improve to other medical image denoising problems. In addition, other multi-resolution analyses can be used to make the denoising scheme more effective. The performance of this study shows the advantage of proposed method: complex version of multi-resolution analyses is very suitable for noise removal from medical images.

REFERENCES

[1] Morlet J., Arehs G., Forugeau I., Giard D., "Wave Propagation and Sampling Theory", Geophysics, vol. 47, pp. 203-236, 1982.  
 [2] Morlet J., Arehs G., "Decompsotition Of Hardy Functions into Square Integrable Wavelets of Constant Shape", SIAM J. Math. Anal., vol. 15, no. 4, p.p. 723-736, 1984.

[3] Chui C. K., Wu S., "An Introduction to Wavelets", Academic Press, 1992.  
 [4] Meyer Y., "Wavelets and Operators", Cambridge Studies in Advanced Mathematics 37 , 1993.  
 [5] Mallat S., "A Theory For Multiresolution Signal Decomposition: The Wavelet Representation", IEEE Trans. Pattern Anal. Machine Intell., vol. 11, p.p. 674-693, 1989.  
 [6] Daubechies I., "Ten Lectures on Wavelets", PA: SIAM , Philadelphia, 1992.  
 [7] Coifman R. R., Wickerhauser M. V., "Entropy Based Algorithms For Best Basis Selection", IEEE Trans. On Information Theory, vol. 38, no. 2, 1992.  
 [8] Lawton W., "Applications of Complex Valued Wavelet Transforms to Subband Decomposition", IEEE Trans. Sig. Proc., vol. 41, no. 12, p.p. 3566-3568,1993.  
 [9] Lina J. M., "Complex Daubechies Wavelets: Filter Design and Applications", Proc.ISAAC Conf., University of Delaware,1997.  
 [10] Lang M., Guo H. and Odegard J. E., "Noise Reduction Using Undecimated Discrete Wavelet Transform", IEEE Signal Processing Letters, 1995.  
 [11] Mojsilovic A., Popovic M., Sevic D., "Classification of The Ultrasound Liver Images with The 2N X 1-D Wavelet Transform", IEEE Int.Conf.Image, vol.1, p.p. 367-370, 1996.

COMPARISON OF REAL AND COMPLEX-VALUED VERSIONS OF WAVELET TRANSFORM,  
CURVELET TRANSFORM AND RIDGELET TRANSFORM FOR MEDICAL IMAGE DENOISING

Huseyin YASAR, Murat CEYLAN, Ayse Elif OZTURK

- [12] Chang S.G., Yu B. and Vattereli M., "Adaptive Wavelet Thresholding for Image Denoising and Compression", *IEEE Trans. Image Processing*, vol. 9, pp. 1532-1546, Sept. 2000.
- [13] Portilla J., Strela V., Wainwright M. J., Simoncelli, E.P., "Adaptive Wiener Denoising using a Gaussian Scale Mixture Model in The Wavelet Domain", *Proceedings of the 8th International Conference of Image Processing Thessaloniki, Greece, October 2001*.
- [14] Chen G. Y. and Bui T. D., "Multi-wavelet De-noising using Neighboring Coefficients", *IEEE Signal Processing Letters*, vol. 10, no. 7, pp. 211-214, 2003.
- [15] Abdulmunim M. E., "Color Image Denoising Using Discrete Multiwavelet Transform", *Department of Computer Science, niversity of Technology, 2004*.
- [16] Benjaminsen C., "Filtering of Periodic Noise Using the Complex Wavelet Transform", *M.Sc. thesis, Informatics and Mathematical Modelling, Technical University of Denmark, DTU, 2007*.
- [17] Candes E., Donoho D. L., "Ridgelets: The Key to High-Dimensional Intermittency", *Phil. Trans. R. Soc. Lond. A.*, vol. 357, p.p. 2495-2509, 1999.
- [18] Do M. N. and Vetterli M., "The Fnite Ridgelet Transform For mage Representation", *IEEE Transactions on Image Processing*, vol. 12, no. 1, pp. 16-28, 2003.
- [19] Candes E. J., Donoho D. L., "Curvelets- A Surprisingly Effective Nonadaptie Representation For Objects With Edges in Curve and Surface Fitting", In: A. Cohen, C. Rabut and L. Schumaker, Editors, *Curves and Surface Fitting: Saint-Malo 1999*, Vanderbilt University Press, Nashville, pp. 105-120, 2000.
- [20] Donoho D. L., Duncan M. R., "Digital Curvelet Transform: Strategy, Implementation and Experiments", *Proceeding of the SPIE on Wavelet Application VII, Orlando, p.p. 12-30, 2000*.
- [21] Candes E.J., Demanet L., Donoho D.L., Ying L., "Fast Discrete Curvelet Transforms", *tech. rep., Applied and Computational Mathematics, California Institute of Technology, pp. 1-44, 2005*.
- [22] Starck J. L., Candes E. J., Donoho D. L., "The Curvelet Transform For Image Denosing", *IEEE Trans. Image Processing.*, vol. 11, p.p. 131-141, 2002.
- [23] Gyaourova A. , Kamath C. and Fodor I. K., "Undecimated Curvelet Transforms For Image Denoising", *Lawrence livermore National Laboratory, Tech. Rep. UCRL-ID-150931, 2002*.
- [24] Sivakumar R., "Denoising of Computer Tomography Images using Curvelet Transform", *ARNP Journal of Engineering and Applied Sciences. February, 2007*.
- [25] Rayudu D. K. V., Murala S. and Kumar V., "Denoising of Ultrasound Images Using Curvelet Transform", *The 2nd International Conference on Computer and Automation Engineering (ICCAE 2010), Singapore, vol. 3, pp. 447-451, 2010*.
- [26] Li C., Liao X. and Yu J., "Complex-Valued Wavelet Network", *Journal of Computer and System Sciences*, vol. 67, pp. 623-632, 2003.
- [27] Shukla P. D., "Complex Wavelet Transforms and Their Applications", *PhD Thesis, The University of Strathclyde, 2003*.
- [28] Fernandes F., "Directional, Shift- nsensitive, Complex Wavelet Transforms With Controllable Redundancy", *PhD Thesis, Rice University, 2002*.
- [29] Strang G. and Hguyen T., "Wavelets and Filter Banks", *Wellesley-Cambridge Press, 1996*.
- [30] Oppenheim A.V. and Lim J.S., "The Importance Of Phase in Signals", *Proc. IEEE*, vol. 69, pp. 529-541, 1981.
- [31] Lorenzetto G. P. and Kovesi P., "A Phase Based Image Comparison Technique", *DICTA99, University of Western Australia, 1999*.
- [32] Driesen J. and Belmasn R., "Time-Frequency Analysis in Power Measurement Using Complex Wavelets", *IEEE Int. Sympo. On Circuits and Systems, ISCAS2002, pp. 681-684, 2002*.
- [33] Lina J.M., "Image Processing With Complex Daubechies Wavelets", *Journal of Math. Imaging and Vision*, vol. 7, pp. 211-223, 1997.
- [34] Bulow T. and Sommer G., "Hypercomplex Signals- A Novel Extension of The Analytic Signal to The Multidimensional Case", *IEEE Transactions on Signal Processing*, vol. 49, pp. 2844-2852, 2001.
- [35] Selesnick I. W., Baraniuk R. G. and Kingsbury N. G., "The Dual-Tree Complex Wavelet Transform", *IEEE Signal Processing Magazine*, vol.22, pp. 123-151, 2005.
- [36] Donoho D.L., "De-Noising by Soft-Thresholding", *IEEE Transactions On Information Theory*, vol. 41, pp. 613-627, 1995.
- [37] Kreis R., "Issues of Spectral Quality in Clinical H-Magnetic Resonance Spectroscopy And



COMPARISON OF REAL AND COMPLEX-VALUED VERSIONS OF WAVELET TRANSFORM,  
CURVELET TRANSFORM AND RIDGELET TRANSFORM FOR MEDICAL IMAGE DENOISING

Huseyin YASAR, Murat CEYLAN, Ayse Elif OZTURK

A Gallery Of Artifacts”, NMR in Biomedecine, vol. 17, no. 6, pp. 361-381, 2004.

[38] Avcibas I., Sankur B. and Sayood, K., “Statistical Evaluation of Image Quality Measures”, Journal of Electronic Imaging, vol. 11, no. 2, pp. 206-223, 2002.

[39] Farrell J. E., “Image Quality Evaluation in Colour Imaging: Vision And Technology”. MacDonald, L.W. and Luo, M.R. (Eds.), John Wiley, pp. 285-313, 1999.

[40] Cadik M. and Slavik P., “Evaluation of Two Principal Approaches to Objective Image Quality Assessment”, 8th International Conference on Information Visualisation, IEEE Computer Society Press, pp. 513-551, 2004.

[41] Nguyen,T.B. and Ziou, D., “Contextual and Non-Contextual Performance Evaluation of Edge

Detectors”, Pattern Recognition Letters, vol. 21, no.9, pp. 805-816, 2000.

[42] Elbadawy O., El-Sakka M. R. and Kamel M. S., “An Information Theoretic Image-Quality Measure”, Proceedings of the IEEE Canadian Conference on Electrical and Computer Engineering, vol. 1, pp. 169-172, 1998.

[43] Dosselmann R. and Yang X. D., “Existing And Emerging Image Quality Metrics”, Proceedings of the Canadian Conference on Electrical and Computer Engineering, pp. 1906-1913, 2006.

[44] Ceylan M., “A New Complex-Valued Intelligent System Design on Evaluating of The Lung mages With Computerized Tomography”, PhD Thesis, Selcuk University, Graduate School of Natural and Applied Sciences, May, 2009

COMPARISON OF REAL AND COMPLEX-VALUED VERSIONS OF WAVELET TRANSFORM,  
CURVELET TRANSFORM AND RIDGELET TRANSFORM FOR MEDICAL IMAGE DENOISING

Huseyin YASAR, Murat CEYLAN, Ayse Elif OZTURK